Environmental Science & Technology

Article

pubs.acs.org/est

Biodegradation and Cometabolic Modeling of Selected Beta Blockers during Ammonia Oxidation

Sandeep Sathyamoorthy,[†] Kartik Chandran,[‡] and C. Andrew Ramsburg*[,†]

[†]Tufts University, Department of Civil and Environmental Engineering, 200 College Avenue Room 113 Anderson Hall, Medford, Massachusetts 02155, United States

[‡]Columbia University, Department of Earth and Environmental Engineering, 500 West 120 Street Room 1045 Mudd Hall, New York, New York 10027, United States

Supporting Information

ABSTRACT: Accurate prediction of pharmaceutical concentrations in wastewater effluents requires that the specific biochemical processes responsible for pharmaceutical biodegradation be elucidated and integrated within any modeling framework. The fate of three selected beta blockers—atenolol, metoprolol, and sotalol—was examined during nitrification using batch experiments to develop and evaluate a new cometabolic process-based (CPB) model. CPB model parameters describe biotransformation during and after ammonia oxidation for specific biomass populations and are designed to be integrated within the Activated Sludge Models framework. Metoprolol and sotalol were not biodegraded by the nitrification enrichment culture employed herein. Biodegradation of atenolol was observed and linked to the activity of ammonia-oxidizing bacteria (AOB) and heterotrophs but not nitrite-oxidizing bacteria. Results suggest that the role of AOB in atenolol degradation may be disproportionately more significant than is otherwise suggested by their lower relative abundance in typical biological treatment processes. Atenolol was observed to competitively inhibit AOB growth in our experiments, though model simulations suggest inhibition is most relevant at atenolol concentrations greater than approximately 200 ng·L^{-1}. CPB model parameters were found to be relatively insensitive to biokinetic parameter selection suggesting the model approach may hold utility for describing pharmaceutical biodegradation during biological wastewater treatment.

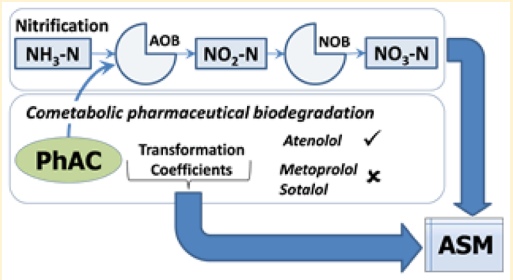

INTRODUCTION

Reports that contemporary pharmaceuticals (PhACs) are present in the natural environment have engendered scientific concern related how these emerging contaminants may influence ecosystem health.[1] Initial toxicological studies suggest that chronic exposure to some PhACs, including beta blockers, at microgram per liter levels may decrease embryo hatching, reduce growth rates in fish, and impact endocrine system activity in aquatic species.[2,3] Wastewater treatment plants (WWTPs) are a primary pathway by which PhACs enter the aquatic environment. While WWTPs are not specifically designed to treat PhACs, several studies highlight attenuation across biological treatment processes.[4−6] Variability in PhAC removals is commonly attributed to molecular structure of the PhAC and operating conditions of the biological treatment process.

Some reports have linked greater PhAC attenuation with longer solids retention times (SRTs ≥ 8−10 day).[6−8] The notion of greater removal at longer SRTs suggests that treatments focused on meeting stringent nutrient requirements may also aid in the attenuation of PhACs, thereby raising interesting questions about the role of nitrifying organisms in PhAC attenuation. It should be recognized, however, that PhAC attenuation in WWTPs operated with longer SRTs could be due to either the presence of slow-growing nitrifying bacteria or more general changes in microbial diversity.[9−15] Many previous studies do not discriminate between PhAC attenuation (i.e., removal) and specific processes leading to attenuation (e.g., sorption, biodegradation, abiotic transformation). Moreover, observations of PhAC biodegradation need to be linked to specific biochemical processes (e.g., ammonia oxidation). Therefore, there is a need for research that elucidates and quantifies the influence of specific bacterial populations (e.g., ammonia oxidizing bacteria) on PhAC biodegradation.

The overall objective of this research was to assess the biodegradation of three beta blockers—atenolol (ATN), metoprolol (MET), and sotalol (SOT)—during nitrification. To accomplish this objective, we employed a combination of batch experiments and mathematical modeling to evaluate and link rates of PhAC biodegradation and ammonia oxidizing bacteria (AOB) growth. We hypothesized that if biodegradation of these beta blockers was observed in our experiments there

Received: July 1, 2013
Revised: October 8, 2013
Accepted: October 10, 2013
Published: October 10, 2013

would be a link between the PhAC biodegradation and ammonia oxidation activity. This hypothesis was based upon the fact that AOB are known to catalyze the oxidation of a wide array of organic compounds.[16−18] The ability of AOB to catalyze nonspecific oxidation of several compounds stems from the broad substrate range of ammonia monooxygenase (AMO).[19] While AOB rely on AMO for ammonia oxidation as part of its energy metabolism,[20] the oxidation of organic compounds by AMO does not result in energy generation. In fact, organic compounds undergoing cometabolic oxidation may reduce the rate of ammonia oxidation by competitively binding to the same catalytic site[21] or an allosteric alternate site[22] on AMO.

MATERIALS AND METHODS

Materials. ATN, MET, and SOT were purchased from Sigma Aldrich (Saint Louis, MO). Properties of each beta blocker are provided in Table S-1 in Supporting Information (SI). Purified water (resistivity ≥18.2 mΩ·cm and total organic carbon (TOC) ≤ 8 ppb) was obtained from a Milli-Q Gradient A-10 station (Millipore, Inc.). All other chemical were purchased from Fisher Scientific and Acros Organics unless noted otherwise (Tables S-2 and S-3 in SI). A sequencing batch reactor (SBR) seeded with activated sludge from a municipal wastewater treatment facility in Massachusetts was used to enrich for test cultures of nitrifying bacteria. Details of the biomass source and enrichment process, which was conducted in the absence of exogenous carbon, are provided in the Nitrification Enrichment Culture section of SI.

Batch Experiments. Each beta blocker was evaluated using separate sets of batch experiments conducted at 22 ± 2 °C. Provided here is an overview of the experimental approach. Details of the protocols used in these experiments are provided in SI. The initial experimental matrix focused on assessing biodegradation during nitrification using four reactors for each beta blocker. We subsequently refer to these assessments as the NIT-EXPTs. NIT-EXPTs comprised four treatments: a control to evaluate ammonia and nitrite-oxidation kinetics in the absence of the beta blocker (NC); a control to assess the biodegradation of the beta blocker (∼15 $\mu g \cdot L^{-1}$) in the absence of ammonia oxidation (NI); and two experimental replicates to evaluate biodegradation of the beta blocker (∼15 $\mu g \cdot L^{-1}$) under nitrifying conditions (NE1 and NE2). Note that the NI treatment employed 30 $mg \cdot L^{-1}$ allylthiourea (ATU), added at the beginning of a two-hour pre-experiment mixing period, to inhibit ammonia oxidation.[23] If beta blocker biodegradation in treatments NE1 and NE2 was observed to be greater than that in treatment NI, the experimental matrix was extended to contain three additional reactors used to assess the influence of nitrite oxidation. In this follow-on assessment, referred to herein as NOX-EXPTs, nitrite oxidation was assessed using three treatments: a control to evaluate nitrite oxidation kinetics in the absence of the beta blocker (NxC) and two experimental replicates (NxE1 and NxE2) to evaluate biodegradation of the beta blocker (∼15 $\mu g \cdot L^{-1}$) under nitrite-oxidizing conditions. Each of the NOX-EXPT treatments contained approximately 30 $mg \cdot L^{-1}$ ATU to inhibit AOB. The initial beta blocker concentration (∼15 $\mu g \cdot L^{-1}$) was selected to ensure quality when quantifying each beta blocker and subsequently estimating model parameters. The lack of observed self-inhibition at this concentration suggests that the concentration is appropriate for the kinetic characterization performed herein. All treatments initially contained approximately 20 $mg\text{-}N \cdot L^{-1}$ of ammonium chloride (NIT-EXPTs) or potassium nitrite (NOX-EXPTs), as well as all essential nutrients. DO was maintained above 4 $mg \cdot L^{-1}$ at all times after biomass addition. With the exception of the addition of ATU and DO (described above), all chemical additions (e.g., nitrogen source, PhAC) were made subsequent to the above-described 2-h mixing period and marked the start of each experiment. Initial conditions for experiments conducted with each beta blocker are described in Table S-4 in SI.

Analytical Methods. ATN, MET, and SOT were quantified by fluorescence detection (Agilent 1321 series FLD) subsequent to isocratic separation of a 50 μL injection at 0.40 $mL \cdot min^{-1}$ using an Agilent Series 1100 HPLC equipped with a Kinetix C-18 column (Phenomenex, 2.1 mm × 150 mm, 100 Å) maintained at 30 °C. The mobile phase comprised acetonitrile (ACN) and an aqueous solution of 0.1% phosphoric acid (PA) mixed at 95 vol % PA for ATN and MET and 88 vol % for SOT. Quantification of ATN was based on FLD excitation wavelength (λ_{EX}) of 235 nm and emission wavelength (λ_{EM}) of 314 nm at a retention time of 3.95 min. For MET and SOT, $\lambda_{EX}/\lambda_{EM}$ were 228/324 nm and 235/319 nm, respectively, and retention times were 4.31 and 2.67 min, respectively. Method detection limits for ATN, MET, and SOT (in picograms on column) were 100, 150, and 150, respectively. Ammonia nitrogen concentrations (S_{NH}) were measured using a colorimetric assay: HACH method 10031[24] with UV absorbance at 655 nm measured using a Perkin-Elmer lambda 25 UV/vis spectrophotometer. Concentration of nitrite (S_{NO2}) and nitrate (S_{NO3}) were quantified using Dionex ICS 2000 Ion Chromatograph system equipped with a Dionex AS-50 autosampler and conductivity detector. Separation was achieved using a Dionex Ionpac AS-18 (4 × 250 mm) with a Dionex AG-18 guard column (4 × 50 mm) and an eluent of 22 mM KOH. Total suspended solids (TSS) and volatile suspended solids (VSS) were measured using methods 2540D and 2540E of Standards Methods, respectively.[25]

DNA Extraction and Quantification. Biomass from each reactor was collected, pelletized, and stored at −80 °C until extracted using MOBio Powersoil isolation kits (MOBIO, Carlsbard, CA) following the manufacturer supplied protocol. Extracted DNA was stored at −80 °C until needed for further analyses. Given the 12−25 h duration of these batch experiments, minimal biomass growth (and related change in measurable gene copies) was anticipated. Therefore, equal volumes of the DNA extracts obtained from the initial (t = 0 h) and a late time sample (ATN: t = 25 h. MET: t = 10 h. SOT: t = 24 h) from each reactor were mixed. This composite DNA sample was then used in the quantitative real time polymerase chain reaction (qPCR). DNA concentration and quality were measured using a using nanodrop lite UV spectrophotometer (Thermofisher Scientific).

qPCR was used to estimate the abundance of total bacteria (EUB), ammonia oxidizing bacteria (AOB), and nitrite oxidizing bacteria (NOB). AOB abundance was measured using the ammonia monooxygenase gene subunit A (amoA).[26,27] Abundance of both *Nitrospira* spp. (NOB-Ns) and *Nitrobacter* spp. (NOB-Nb) were measured by targeting the 16s rRNA gene (NOB-Ns;[28] NOB-Nb[29]). Total eubacterial (EUB) abundance was measured using 16s rRNA gene targeted primers.[27,30] In addition to providing estimates of gene copy concentrations, qPCR data were used to estimate biomass concentrations (in $mg\text{-}COD \cdot L^{-1}$). The concentration of heterotrophic bacteria (HET) for each experiment was

Table 1. Model Parameters Used in the Process Model Developed in This Research[a]

description	variable	unit of measure	literature values (where applicable) range	refs.	selected value
Common					
nitrogen fraction of biomass	i_{NBM}	(mg-N·mg-COD^{-1})	0.07	36, 39	0.07
biomass VSS to biomass COD ratio	f_{CV}	(mg-COD·mg-VSS^{-1})	1.42	36, 39	1.42
AOB Kinetics and Stoichiometry					
max. specific growth rate	$\mu_{max,AOB}$	(day^{-1})	0.2−1.6	59	0.50
decay rate	b_{AOB}	(day^{-1})	0.06−0.4	59, 60	0.15
half saturation value for S_{NH}	K_{NH}	(mg-N·L^{-1})	0.14−2.3	61, 62	0.50
ammonia-N yield	Y_{AOB}	(mg-COD·mg-N^{-1})	0.11−0.21	38, 59, 63	0.15
PhAC inhibition coefficient	$K_{I,PhAC-AOB}$	(μgL^{-1})	NA	NA	fit[b]
NOB Kinetics and Stoichiometry					
max. specific growth rate	$\mu_{max,NOB}$	(day^{-1})	0.2−2.6	50	0.50
decay rate	b_{NOB}	(day^{-1})	0.08−1.7	50, 64	0.15
half saturation value for S_{NO2}	K_{NO2}	(mg-N·L^{-1})	0.05−3	60, 65, 66	0.50
nitrite-N yield	Y_{NOB}	(mg-COD·mg-N^{-1})	0.06−0.10	63	0.09
Initial Biomass Concentrations					
AOB	$X_{AOB,t0}$	(mg-COD·L^{-1})	NA	NA	fit[a]
NOB	$X_{NOB,t0}$	(mg-COD·L^{-1})	NA	NA	fit[a]
HET	$X_{HET,t0}$	(mg-COD·L^{-1})	NA	NA	calculated
PhAC Biodegradation					
AOB Transformation Coefficient	$T_{PhAC-AOB}$	(L·g-COD^{-1})	NA	NA	fit[b]
AOB endogenous transformation coefficient	$k_{PhAC-AOB}$	(L·g-COD^{-1}·d^{-1})	NA	NA	fit[b]
HET lumped biodegradation coefficient	$\alpha_{PhAC-HET}$	(L·g-COD^{-1}·d^{-1})	NA	NA	fit[c]

[a] $X_{AOB,t0}$ and $X_{NOB,t0}$: independent, fit using the nitrification control (NC) data. [b] $T_{PhAC-AOB}$, $k_{PhAC-AOB}$, and $K_{I,PhAC-AOB}$: independent, fit using the nitrification experiments (NE1 and NE2) data. [c] $\alpha_{PhAC-HET}$: independent, fit using the nitrification inhibition control (NI) data.

determined as the difference between estimates of total bacteria and nitrifying bacteria. This conversion along with other qPCR details are described in the qPCR Methods section of SI.

MATHEMATICAL MODELING

Model Framework. Two approaches to model PhAC biodegradation were evaluated in this research: (i) pseudo-first-order models based upon VSS concentration and (ii) a cometabolic process-based model. The pseudo-first-order approach (eq 1) is frequently used to model microconstituent biodegradation despite its lack of mechanistic or process significance.[6,14,31,32]

$$\frac{dS_{PhAC}}{dt} = -(k_{BIO}X_{TOT})S_{PhAC} \quad (1)$$

Here, S_{PhAC} is the PhAC concentration [M_{PhAC} L^{-3}], k_{BIO} [L^3 $M_{BIOMASS}^{-1}$ T^{-1}] is a biomass normalized pseudo-first-order biodegradation rate coefficient, X_{TOT} [$M_{BIOMASS}$ L^{-3}] is the biomass concentration, and t [T] is time. Although such a formulation is convenient, it is of limited value when comparing systems with different design or operating conditions. The principal shortfall of this approach is that it does not link PhAC biodegradation to a specific consortium (e.g., AOB, NOB, HET) or specific processes occurring within the mixed community (e.g., ammonia oxidation).

To address this shortcoming, existing approaches for cometabolic biodegradation modeling[33−35] were adapted herein to link PhAC biodegradation to specific biomass biokinetics. The resulting cometabolic process-based (CPB) model was developed and integrated into the Activated Sludge Models (ASM) framework[36] with nitrification modeled as a two-step process[37,38] (SI Table S-9). A detailed development of the model is provided in the Cometabolic Process-Based Model Development section of SI. In brief, the basis for the cometabolic process-based model is the concept of growth-based transformation capacity, which is described by Criddle[34] as the mass of nongrowth substrate transformed per unit mass of growth substrate consumed during growth [M_{NGS} M_{GS}^{-1}]. This transformation capacity is modified by Monod type expressions for the nongrowth and growth substrates.[34] Here, we modify the concept of transformation capacity to produce a transformation coefficient [L^3 M_{COD}^{-1}] that facilitates integration of the CPB model into the ASM framework employing biomass growth as a process rate [L^3 $M_{COD}^{-1}T^{-1}$] (SI Table S-9). Based upon the observation that typical half saturation values for solutes in environmental systems are several orders of magnitude greater than our applied concentration of PhAC (15 μgL^{-1}),[33,39,40] we assume that the cometabolic model is first-order with respect to PhAC concentration. The resulting cometabolic model (eq 2) is used within the ASM framework to assess three processes contributing to PhAC biodegradation: (i) cometabolic biodegradation linked to AOB growth, (ii) biodegradation by AOB in the absence of growth, and (iii) biodegradation due to HET present in the mixed culture.

$$\frac{dS_{PhAC}}{dt} = -\left\{\begin{matrix}(T_{PhAC-AOB}\mu_{AOB} & + & k_{PhAC-AOB})X_{AOB} \\ + (T_{PhAC-HET}\mu_{HET} & + & k_{PhAC-HET})X_{HET}\end{matrix}\right\}S_{PhAC} \quad (2)$$

Here, $T_{PhAC-AOB}$ is a cometabolic PhAC transformation coefficient linked to AOB growth during ammonia oxidation [L^3 M_{COD}^{-1}], μ_{AOB} is the specific growth rate of AOB [T^{-1}], $k_{PhAC-AOB}$ is a biomass normalized PhAC biodegradation rate coefficient in the absence of ammonia oxidation [L^3 M_{COD}^{-1} T^{-1}], and X_{AOB} is the AOB concentration [M_{COD} L^{-3}]. Similarly, $T_{PhAC-HET}$ is a cometabolic PhAC transformation coefficient linked to HET growth [L^3 M_{COD}^{-1}], μ_{HET} is the specific growth rate of HET [T^{-1}], $k_{PhAC-HET}$ is a biomass

normalized PhAC biodegradation rate coefficient in the absence of HET growth substrate [L^3 $M_{COD}{}^{-1}T^{-1}$], and X_{HET} is the HET concentration [M_{COD} L^{-3}]. S_{PhAC} is the PhAC concentration [M_{PhAC} L^{-3}].

Given our focus on nitrification, the growth of HET was not modeled. Instead, we assume growth of HET over the experimental period was small enough that X_{HET} remained approximately constant over the course of the experiment. This assumption is supported by the fact that the nitrification enrichment SBR (source of the biomass used in the experiments) was operated for over 100 days with no addition of exogenous carbon, and the only exogenous organic carbon added to the batch reactors was the ∼15 μgL^{-1} PhAC. Furthermore, the rate at which endogenous organic carbon becomes available is effectively constrained by the rate of biomass decay (taken to be 0.15 day^{-1}, Table 1). Based upon the assumption of limited HET growth during the experiments, eq 2 was modified to contain a single biomass normalized rate coefficient to describe the influence of HET on the PhAC, $\alpha_{PhAC\text{-}HET}$ [L^3 $M_{COD}{}^{-1}$ T^{-1}] (eq 3).

$$\frac{dS_{PhAC}}{dt} = -\left\{\begin{array}{l}(T_{PhAC-AOB}\mu_{AOB} \quad + \quad k_{PhAC-AOB})X_{AOB} \\ + \ (\alpha_{PhAC-HET})X_{HET}\end{array}\right\}S_{PhAC} \tag{3}$$

It is important to note that the model framework proposed here is flexible and readily adapted as estimates for $T_{PhAC\text{-}HET}$ and $k_{PhAC\text{-}HET}$ become available.

Model Solution. The modeling objective herein was estimation of values for $T_{PhAC\text{-}AOB}$, $k_{PhAC\text{-}AOB}$, and $\alpha_{PhAC\text{-}HET}$ for the selected beta blockers. The mathematical model used in this research (SI Table S-11) comprises six, coupled, ordinary differential equations—one each for X_{AOB}, X_{NOB}, S_{NH}, S_{NO2}, S_{NO3}, and S_{PhAC}—and 17 parameters (Table 1). Parameter estimation was accomplished in MATLAB (Mathworks, release 2010b) using the *lsqnonlin* routine with a Levenberg−Marquardt algorithm in a sequential solution strategy, as described below. In each model run, the model equations were solved using an explicit time discretized Runge−Kutta 1 method with a time-step of 30 s implemented in MATLAB. The 95% confidence intervals for all estimated parameters were determined using the *nlparci* routine.

To minimize the number of adjustable parameters in any one fit, the initial concentrations of AOB ($X_{AOB,t0}$) and NOB ($X_{NOB,t0}$) were first independently estimated for each experiment (e.g.,. ATN, MET, SOT) using data from the nitrification control (NC). Values of $X_{AOB,t0}$ and $X_{NOB,t0}$ were constrained between 1.0 mg-COD·L^{-1} and the COD equivalent of the measured VSS concentration. The fits producing the lowest sum of square errors (SSE) between measured and modeled values of S_{NH}, S_{NO2}, and S_{NO3} determined $X_{AOB,t0}$ and $X_{NOB,t0}$. $X_{AOB,t0}$ and $X_{NOB,t0}$ were subsequently employed for all simulations of nitrification in the presence of the given PhAC (i.e., treatments NI, NE1, and NE2).

Values of $\alpha_{PhAC\text{-}HET}$ were independently estimated for each experiment using data from the nitrification inhibition control reactor (NI). Here, X_{HET} was fixed as the difference between the total bacteria and nitrifying bacteria concentrations produced from the qPCR results. PhAC data from the NI treatments were fit by adjusting values of $\alpha_{PhAC\text{-}HET}$ with $T_{PhAC\text{-}AOB}$ and $k_{PhAC\text{-}AOB}$ set to zero such that the SSE between the measured and modeled S_{PhAC} was minimized. It is recognized that assuming $T_{PhAC\text{-}AOB}$ and $k_{PhAC\text{-}AOB}$ are zero here means any residual biodegradation capacity of the inhibited AOB will be lumped into the estimate of heterotrophic biodegradation. The influence of this assumption is negligible since ATU binds with copper at the AMO active site to inhibit its activity[41] and thus dramatically limits residual activity.

Estimates of $X_{AOB,t0}$ and $X_{NOB,t0}$ and $\alpha_{PhAC\text{-}HET}$ obtained from the NC and NI treatments, respectively, were then employed with nitrogen and PhAC concentration data from treatments NE1 and NE2 to estimate PhAC biodegradation. Data from the replicate reactors (NE1 and NE2) were used together in a single fit to produce values of $T_{PhAC\text{-}AOB}$ and $k_{PhAC\text{-}AOB}$ by minimizing the SSE between the measured and modeled S_{PhAC}.

RESULTS AND DISCUSSION

Microbial Community Structure. qPCR results suggest that AOB are dominant in the enrichment community and represent between 75% and 85% of the nitrifying population (i.e., AOB + NOB) (Figures S-1 and S-2 in SI). These data are consistent with previous studies of nitrifying populations in systems treating high nitrogen loads.[42] *Nitrobacter* spp. are dominant NOB, effectively accounting for the remainder of the nitrifying population. *Nitrospira* spp. account for less than 0.1% of the nitrifying population. This observation can be explained due to the high S_{NH} concentrations used in the nitrification enrichment SBR, which was the seed biomass source for these experiments. High levels of S_{NH} result in high S_{NO2} levels during the SBR cycle, which favors *Nitrobacter* over *Nitrospira* NOB.[43] Estimates of HET suggest they represent <25% of the community.

Beta Blocker Biodegradation. Results indicate that MET are SOT not attenuated in the presence of this nitrification enrichment community (Figures S-4 and S-5 in SI). In contrast, ATN was attenuated by approximately 30% in the experimental reactors (i.e., ATN treatments NE1 and NE2) before S_{NH} fell below 0.2 mg-N·L^{-1} around 4 h (Figure 1). Interestingly, ATN was further attenuated by approximately 50% after nitrification was complete (i.e., ∼80% of the ATN was attenuated after 25 h) (Figure 1). In comparison, the extent of ATN attenuation in the nitrification inhibition control (i.e., ATN treatment NI) at the completion of the 25 h experiment reactor is 30% (Figure 1). Attenuation of ATN during nitrite oxidation (NOX-EXPTs) was also explored in an attempt to elucidate the biochemical processes in nitrification that may contribute to the observed attenuation. Results from this NOX-EXPT (Figure S-6 in SI) indicate that ATN attenuation was approximately 30% over the 25 h experimental duration. The lack of quantifiable attenuation in the SOT and MET NIT-EXPTs is consistent with distribution coefficients measured for these beta blockers that indicate sorption has a negligible influence on attenuation (SI Figure S-3 and refs 44 and 45). Thus, ATN attenuation was attributed to biological activity even in the absence of direct evidence (i.e., observation of biodegradation products). Taken in concert these results suggest (i) ammonia oxidation may have a role in supporting ATN degradation and (ii) the biodegradability of PhACs from the same therapeutic family or having similar chemical structures by nitrifying bacteria may be substantially different.

The biomass normalized, pseudo-first-order biodegradation rate coefficient for ATN in the experimental replicates, $k_{BIO\text{-}ATN,NIT}$ is 2.39 ± 0.21 L·g-VSS^{-1}·d^{-1} (1.68 ± 0.15 L·g-COD^{-1}·d^{-1}) (Table 2). The analogous coefficient under nitrification inhibition conditions ($k_{BIO\text{-}ATN,NIT\text{-}INH}$) is 0.56 ±

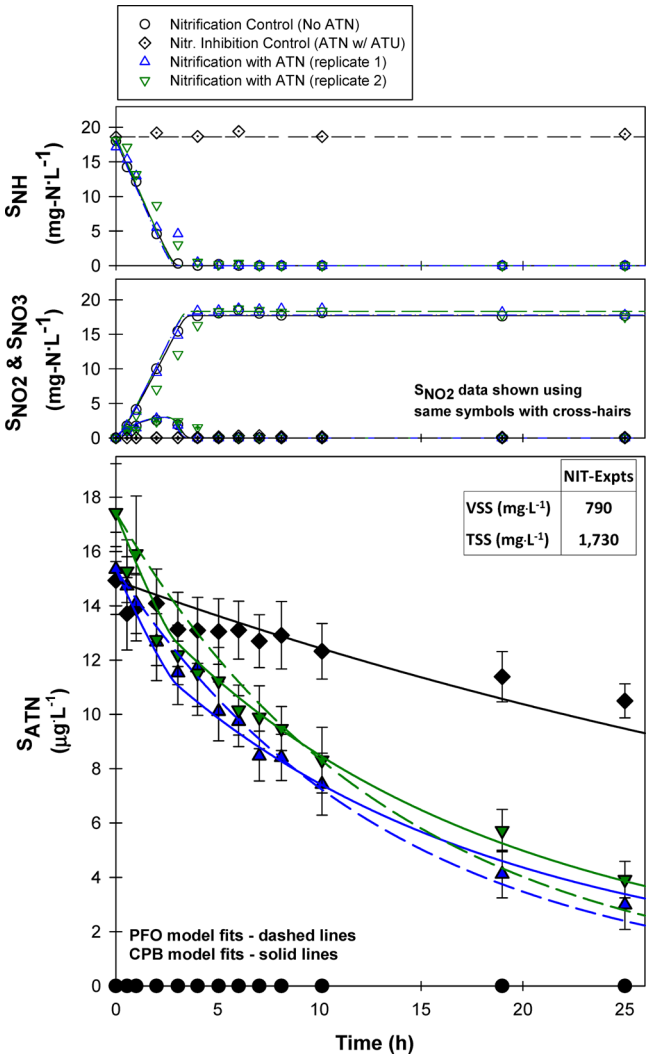

Figure 1. Observed and modeled concentrations of ammonia (top panels), nitrite and nitrate (middle panels), and ATN (bottom panel) for NIT-EXPTs conducted with ATN. Results are shown from each of the four NIT-EXPT reactors: a nitrification control (○ NC), a nitrification inhibition control (◊ NI), and replicate experimental reactors (△ NE1 and ▽ NE2). Open symbols denote nitrogen species and filled symbols denote ATN. Also shown are PFO model (dashed lines) and CPB model (solid lines) fits of the data. Note that the PFO model is not capable of simulating nitrification and thus does not appear in the top and middle panels. Model parameters are provided in Table 2.

0.10 L·g-VSS^{-1}·d^{-1} (0.40 ± 0.07 L·g-COD^{-1}·d^{-1}). The biodegradation rate of ATN when nitrification is not inhibited is therefore approximately four times greater than when nitrification is inhibited by ATU. This is consistent with the hypothesis that the activity of nitrifying bacteria controls the biodegradation of ATN in this nitrification enrichment community. It is important to note here that the highest nitrite concentration observed was less than 5 mg-N·L^{-1}, which suggests nitration reactions are not relevant in our experiments.[46] No production of either nitrite or nitrate was observed in the nitrification inhibition control, which indicates the utility of the ATU addition. The biomass normalized pseudo-first-order order biodegradation rate coefficient for ATN during nitrite oxidation (ATN treatments NxE1 and NxE2, in the absence of ammonia oxidation) is 0.39 ± 0.05 L·g-VSS^{-1}·d^{-1}. This is less than rate coefficient obtained from the ATN nitrification experiments NE1 and NE2 (2.39 ± 0.21 L·g-VSS^{-1}·d^{-1}) and consistent with that observed when nitrification was inhibited with ATU (0.56 ± 0.10 L·g-VSS^{-1}·d^{-1} in NI).

The rate coefficient for ATN biodegradation during nitrification, when converted to a suspended solids normalized value (1.09 ± 0.10 L·g-SS^{-1}·d^{-1}) is comparable to those reported by Maurer et al.[45] (0.98 L·g-SS^{-1}·d^{-1} in batch experiments using biomass from an MBR operated at 20 day SRT) and Wick, et al.[47] (1.90 and 1.10 L·g-SS^{-1}·d^{-1} in batch experiments using sludge from a suspended growth system operated at 18 day SRT). The similarity between these reported rate coefficients is noteworthy considering that the comparison includes experiments conducted with biomass from a nitrification enrichment (SBR operated at >100 d SRT) containing a relatively low fraction of heterotrophs (~20%), and biomass from WWTPs operating at 18−20 d SRT. Interestingly, and in contrast to our results, both Maurer et al. and Wick et al. reported attenuation of MET (0.82 L·g-SS^{-1}·d^{-1}, and 0.38 L·g-SS^{-1}·d^{-1}, respectively) and SOT (0.41 L·g-SS^{-1}·d^{-1} and 0.42 L·g-SS^{-1}·d^{-1}, respectively). While these studies imply PhAC biodegradation occurred due to nitrification processes, neither Maurer et al. nor Wick et al. report concentrations of nitrogen species or attempt to link PhAC biodegradation to specific biological processes. Thus, there is no way to assess if the observation of MET and SOT biodegradation in these studies resulted from nitrification or heterotrophic activity.

A preliminary assessment of the ATN biodegradation rate during and after nitrification suggests that two distinct processes may be occurring. We explored this in a simplified way by extending the pseudo-first-order model to a dual rate, pseudo-first-order model (see SI for details). Interestingly,

Table 2. ATN Biodegradation Parameters for the PFO and CPB Models Evaluated in This Research[a]

pseudo-first-order (PFO) model parameters	$k_{BIO\text{-}ATN,NIT}$	1.68 ± 0.15	L·g-COD^{-1}·d^{-1}
	$k_{BIO\text{-}ATN,NIT\text{-}INH}$	0.40 ± 0.07	L·g-COD^{-1}·d^{-1}
cometabolic process based (CPB) model parameters	$T_{ATN\text{-}AOB}$	71.5 ± 22.7	L·g-COD^{-1}
	$k_{ATN\text{-}AOB}$	16.1 ± 5.6	L·g-COD^{-1}·d^{-1}
	$\alpha_{ATN\text{-}HET}$	22.4 ± 4.4	L·g-COD^{-1}·d^{-1}
improvement in model performance when using CPB model			
$\Delta SSE_{NE1+NE2}$	−9.1		
$\Delta AIC_{C,NE1+NE2}$	−19.5		

[a]Also provided is the improvement in model performance for the experimental reactors with ATN (NE1 and NE2) when using the CPB model (as described by decreases in SSE and AIC_C).

when the extended pseudo-first-order model is made population specific (i.e., pseudo-first-order rates for HET and AOB), it offers a similar description of the data as the pseudo-first-order model (see SSE and Nash−Sutcliffe Efficiency in SI Table S-10). Thus, the small sample corrected Akaike Information Criteria (AICc)[48] suggests that the addition of the second fitting parameter is not warranted for the pseudo-first-order approach. It is important to recognize the extended pseudo-first-order models (SI equations S6 and S7) assume that AOB remain active over the duration of the experiment. As noted above, this may be inappropriate (S_{NH} is <0.2 mg-N·L^{-1} after 4 h) and highlights the need for a process based model.

Cometabolic Process-Based Model. Data from the NC treatment with each PhAC were used to estimate the initial AOB and NOB concentrations ($X_{AOB,t0}$ and $X_{NOB,t0}$). Model fit values of $X_{AOB,t0}$ and $X_{NOB,t0}$ (SI Table S-7) appear to fall within the generally accepted level of accuracy for biomass concentrations estimated using qPCR (i.e., up to ±100%).[49,50] Nitrogen data and process model simulations for the MET, SOT, and ATN NIT-EXPTs are shown in SI Figures S-4, S-5 and Figure 1, respectively. Note that the composition of the initial biomass employed for each NIT-EXPT is fit using the nitrification control data for each beta blocker. Simulations shown for NI, NE1, and NE2 for MET and SOT are predictions using the fitted initial biomass concentrations (SI Table S-7) and model parameters (Table 1). When this procedure was conducted for the experimental reactors containing ATN, the S_{NH} residuals were observed to be larger at low S_{NH} suggesting that the model may be unable to satisfactorily predict S_{NH} oxidation as S_{NH} approaches the half saturation value. This effect was not observed with MET or SOT as visual differences in the nitrogen data with either MET or SOT present are attributable to minor differences in measured initial ammonia concentration in treatments NC, NE1, and NE2. To explore the hypothesis that ATN exerts a competitive inhibition on AOB growth, the AOB growth process rate ($r_{G,X_{AOB}}$) was modified as shown in eq 4[51] and the nitrification data from the experimental reactors (ATN treatments NE1 and NE2) were fit by adjusting a single parameter, $K_{I,ATN\text{-}AOB}$.

$$r_{G,X_{AOB}} = \left[\mu_{max,AOB}\left(\frac{S_{NH}}{K_{NH}\left(1+\frac{S_{ATN}}{K_{I,ATN-AOB}}\right)+S_{NH}}\right)\right]X_{AOB} \quad (4)$$

Application of the competitive inhibition model significantly improved model performance when $K_{I,ATN\text{-}AOB}$ = 1.84 ± 0.39 μg·L^{-1} (Figure 2, SSE reduced to 39% and 15% and AIC_C reduced to 37% and 79% of the base case values for NE1 and NE2, respectively). These data and simulations strongly suggest that ATN may competitively inhibit the ammonia oxidation process, which is consistent with the hypothesis of cometabolic degradation due to AMO. That notwithstanding, the possibility that biodegradation products contribute to the observed inhibition[52] cannot be eliminated even though none were observed in our experiments. This is, as far as we are aware, the first report of possible PhAC inhibition of ammonia oxidation. Thus, we encourage subsequent studies to consider the possibility of inhibition and, where possible, give greater emphasis to establishing the mode(s) of inhibition.

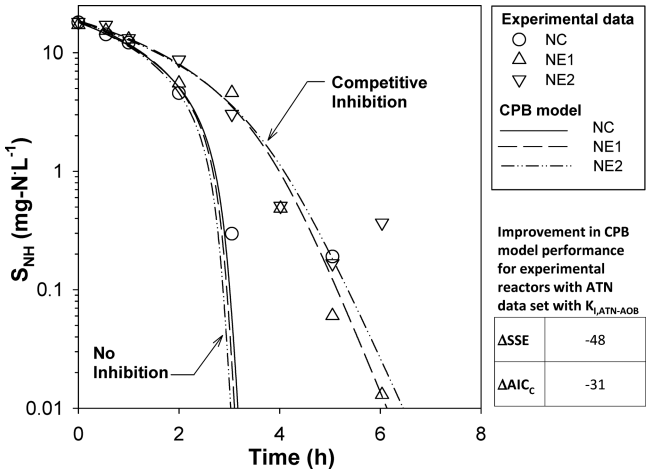

Figure 2. Observed and modeled concentration of ammonia during the ATN experiment. Data are shown for a nitrification control reactor (NC) and experimental replicates (NE1 and NE2). Note that minor differences between the simulations for the experimental replicates (in both the inhibition and no inhibition simulations) entirely result from subtle differences in the measured initial S_{NH} concentrations in each reactor. Simulations shown include the two-step nitrification model with and without competitive inhibition. The competitive inhibition is described by eq 4 with $K_{I,ATN\text{-}AOB}$ = 1.84 ± 0.39 μg·L^{-1}. The combined improvement in the fit for data from NE1 and NE2 when using the competitive inhibition model is shown by the decreases in SSE and AIC_C from those obtained when the data are modeled without competitive inhibition.

With the competitive inhibition model for ammonia oxidation model in place, the transformation capacity for ATN can be assessed. To accomplish this, the process model was first fit to the nitrification inhibition data to determine that $\alpha_{ATN\text{-}HET}$ = 22.4 ± 4.4 L·g-COD^{-1}·d^{-1}. Best fit values of $T_{ATN\text{-}AOB}$ and $k_{ATN\text{-}AOB}$ were subsequently determined using the replicate experimental reactors to be 71.5 ± 22.7 L·g-COD^{-1} and 16.1 ± 5.6 L·g-COD^{-1}·d^{-1}, respectively. Comparison of the values of $T_{ATN\text{-}AOB}$ or $k_{ATN\text{-}AOB}$ to similarly estimated values for other PhACs is not currently possible due to the nearly universal practice of modeling PhAC attenuation using a single, pseudo-first-order rate coefficient. Note, however, that the performance of cometabolic process rate model is markedly greater than any pseudo-first-order approach (see goodness of fit metrics in SI Table S-10) and illustrates the merit of linking PhAC biodegradation to specific biochemical processes. Since this is the first known cometabolic modeling of PhAC biodegradation, we endeavored to compare our results for ATN with reported cometabolic biodegradation of conventional organic pollutants by AOB in axenic or mixed nitrifying communities.[53−56] It is, however, important to note here that the nomenclature within the cometabolic literature is quite diverse as a result of (i) differences in bases for normalization (e.g., biomass normalized vs growth substrate normalized), and, more importantly, (ii) similarity in terminology used to describe different mechanisms (e.g., transformation capacity is used to describe biodegradation in the presence and absence of growth). This makes difficult the direct comparison of our measured transformation coefficients ($T_{ATN\text{-}AOB}$ and $k_{ATN\text{-}AOB}$) to previous studies. One set of parameters that align with our modeling approach are those of Kocamemi and Cecen[56] for the cometabolic biodegradation of TCE by AOB in a mixed biomass community (equivalent values of $T_{TCE\text{-}AOB}$ and

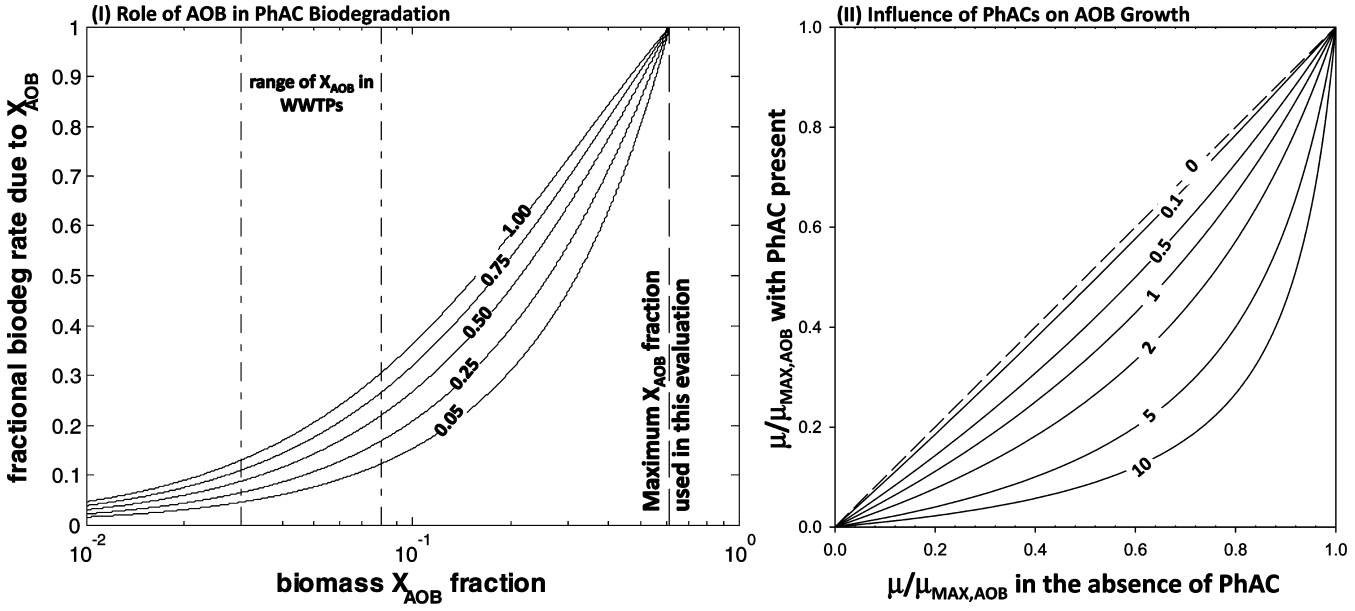

Figure 3. Left: Contribution of ammonia oxidizing bacteria to the rate of ATN biodegradation (i.e., fractional biodegradation rate resulting due to X_{AOB}) as a function of fraction of AOB in the biomass. Each curve represents a specific condition related to ammonia concentration (and operating conditions) resulting in a given AOB growth rate relative to the maximum specific growth rate. Note that AOB are assumed to constitute approximately 60% of the nitrifying bacteria, which is therefore the maximum X_{AOB} fraction (vertical dashed line) when all the biomass is made up of nitrifying bacteria. Right: Influence of PhAC inhibition on AOB growth. Each curve represents the ratio of the PhAC concentration to the inhibition coefficient ($K_{I,PhAC\text{-}AOB}$).

$k_{TCE\text{-}AOB}$ are ~50 ± 17 L·g-COD^{-1} and ~7 ± 1 L·g-COD^{-1}·d^{-1}, respectively, see ref 57). However, given the marked difference in molecular properties between TCE and ATN, caution is warranted when considering comparisons between the cometabolic rate parameters for these compounds.

Monte Carlo (MC) simulations were conducted to evaluate the sensitivity of the fitted values of $X_{AOB,t0}$, $X_{NOB,t0}$, $\alpha_{ATN\text{-}HET}$, $T_{ATN\text{-}AOB}$, $k_{ATN\text{-}AOB}$, and $K_{I,ATN\text{-}AOB}$ on the selected values of the growth parameters $\mu_{MAX,AOB}$, b_{AOB}, K_{NH}, $\mu_{MAX,NOB}$, b_{NOB}, and K_{NO2}. Methods for and results from the 2000 MC simulations are detailed in SI. Results suggest that the range (5−95th percentile values) of $T_{ATN\text{-}AOB}$ and $k_{ATN\text{-}AOB}$ are 66.3−73.0 L·g-COD^{-1} and 8.6 to 45.5 L·g-COD^{-1}·d^{-1}, respectively (Table S-12 in SI). $T_{ATN\text{-}AOB}$ is therefore relatively insensitive to selection of AOB growth parameters (Figure S-7 in SI). The greater variation in $k_{ATN\text{-}AOB}$ can be explained by the role of $\mu_{MAX,AOB}$ in the model (Figure S-8 in SI). At high values of $\mu_{MAX,AOB}$, the duration over which $T_{ATN\text{-}AOB}$ contributes to ATN biodegradation is shorter (i.e., shorter period for ammonia oxidation). Thus, we hypothesize that the apparent relationship between $k_{ATN\text{-}AOB}$ and $\mu_{MAX,AOB}$ reflects the need for higher $k_{ATN\text{-}AOB}$ (at higher $\mu_{MAX,AOB}$) when fitting the experimental data. The ATN inhibition constant ($K_{I,ATN\text{-}AOB}$) varies from 1.18 to 8.86 μg·L^{-1} (recall that for the CPB model with inhibition $K_{I,ATN\text{-}AOB}$ = 1.84 ± 0.39 μg·L^{-1}). The estimated range of $K_{I,ATN\text{-}AOB}$ (~4−33 nM) is significantly lower than inhibition coefficients reportedly exerted by chlorinated solvents in pure *N. europaea* cultures (~12−1000 μM) suggesting that the affinity of AMO for ATN may be significantly greater. Results from the MC sensitivity analysis suggest that CPB model developed in this research may hold more general utility for describing PhAC biodegradation, especially given the widespread usage of the ASM modeling framework in industrial WWTP process simulators (e.g., Biowin, GPSx, etc.).

Implications. Results of our experiments indicate that ATN biodegradation resulted from ammonia oxidation. If the rate of degradation by HET quantified here in the absence of exogenous carbon is indicative of the rate expected when carbon is more readily accessible (e.g., BOD in influent of a plant), the role of AOB in ATN biodegradation may be more relevant than previously estimated. It is conventionally assumed that the role of nitrifying bacteria in PhAC biodegradation is limited by the small number fraction of these organisms in the biomass at a WWTP. Our research suggests that even when AOB make up 5% of the total biomass in a WWTP reactor, they contribute between 7−17% to the biodegradation rate of ATN (Figure 3, left panel). That is to say, their contribution outweighs their proportion in the biomass. This implication may be particularly relevant for partial nitrification processes (e.g., SHARON) where AOB make up greater than 10% of the biomass.[58] Equally important is the inhibition of AOB observed in our experiments. Where ATN is present, even at half the inhibition coefficient value, the maximum achievable growth rates are significantly reduced (Figure 3, right panel). Moreover, the influence may need to be summed over multiple inhibitors given the additive nature of this type of inhibition[41] and the many microconstituents present in wastewater. Therefore, based on this study, any inhibition of AOB may not only reduce the ability of WWTPs to meet stringent effluent nitrogen targets—a significant focus of modern WWTPs—but may also negatively influence PhAC biodegradation due to the reduction in the growth rate of AOB (Figure 3, right panel).

■ ASSOCIATED CONTENT

Supporting Information

Properties of beta blockers used in this research, details related to nitrification enrichment, batch experiment protocols, qPCR methods and results, time course data for nitrogen species and

beta blocker from each experiment. This material is available free of charge via the Internet at http://pubs.acs.org.

AUTHOR INFORMATION

Corresponding Author

*Phone: 617-627-4286. Fax: 617-627-3994. E-mail: andrew.ramsburg@tufts.edu.

Notes

The authors declare no competing financial interest.

ACKNOWLEDGMENTS

The authors wish to acknowledge Dr. David Stensel (University of Washington) for suggestions related to influence of pharmaceuticals on nitrification processes, Dr. Steven Chapra (Tufts University) for recommendations related to the Monte Carlo simulations, and Dr. Natalie Cápiro (Tufts University) for initial suggestions related to qPCR analyses. The authors are grateful to Mr. Scott Rossi for providing the seed sludge for the nitrification enrichment SBR. Appreciation is also expressed to the four anonymous reviewers who helped to improve this manuscript. Partial support was provided by the Massachusetts Water Resources Research Center under grant number 2011MA291B. Additional support was provided by Tufts University in the form of Faculty Research Awards Committee grant to C.A.R. and a Graduate Student Award to S.S. Partial support for the lab-scale SBR system was provided by AECOM. Any opinions, findings, and conclusions or recommendations expressed in this material are those of the authors and do not necessarily reflect the views of the sponsors.

REFERENCES

(1) Daughton, C. H.; Ternes, T. A. Special Report: Pharmaceuticals and personal care products in the environment: Agents of subtle change? (vol 107, pg 907, 1999). *Environ. Health Perspect.* **2000**, *108*, 598−598.

(2) Ings, J. S.; George, N.; Peter, M. C. S.; Servos, M. R.; Vijayan, M. M. Venlafaxine and atenolol disrupt epinephrine-stimulated glucose production in rainbow trout hepatocytes. *Aquat. Toxicol.* **2012**, *106*, 48−55.

(3) Massarsky, A.; Trudeau, V. L.; Moon, T. W. Beta-blockers as endocrine disruptors: The potential effects of human beta-blockers on aquatic organisms. *J. Exp. Zool. Part A* **2011**, *315A* (5), 251−265.

(4) Bendz, D.; Paxeus, N. A.; Ginn, T. R.; Loge, F. J. Occurrence and fate of pharmaceutically active compounds in the environment, a case study: Hoje River in Sweden. *J. Hazard. Mater.* **2005**, *122* (3), 195−204.

(5) Ternes, T. A. Occurrence of drugs in German sewage treatment plants and rivers. *Wat. Res.* **1998**, *32* (11), 3245−3260.

(6) Joss, A.; Zabczynski, S.; Gobel, A.; Hoffmann, B.; Loffler, D.; McArdell, C. S.; Ternes, T. A.; Thomsen, A.; Siegrist, H. Biological degradation of pharmaceuticals in municipal wastewater treatment: Proposing a classification scheme. *Water Res.* **2006**, *40* (8), 1686−96.

(7) Clara, M.; Kreuzinger, N.; Strenn, B.; Gans, O.; Kroiss, H. The solids retention time—A suitable design parameter to evaluate the capacity of wastewater treatment plants to remove micropollutants. *Water Res.* **2005**, *39* (1), 97−106.

(8) Kreuzinger, N.; Clara, M.; Strenn, B.; Kroiss, H. Relevance of the sludge retention time (SRT) as design criteria for wastewater treatment plants for the removal of endocrine disruptors and pharmaceuticals from wastewater. *Water Sci. Technol.* **2004**, *50* (5), 149−156.

(9) Reif, R.; Suarez, S.; Omil, F.; Lema, J. M. Fate of pharmaceuticals and cosmetic ingredients during the operation of a MBR treating sewage. *Desalination* **2008**, *221* (1−3), 511−517.

(10) Tran, N. H.; Urase, T.; Kusakabe, O. The characteristics of enriched nitrifier culture in the degradation of selected pharmaceutically active compounds. *J. Hazard. Mater.* **2009**, *171* (1−3), 1051−1057.

(11) Suarez, S.; Lema, J. M.; Omil, F. Removal of pharmaceutical and personal care products (PPCPs) under nitrifying and denitrifying conditions. *Water Res.* **2010**, *44* (10), 3214−24.

(12) Batt, A. L.; Kim, S.; Aga, D. S. Enhanced biodegradation of iopromide and trimethoprim in nitrifying activated sludge. *Environ. Sci. Technol.* **2006**, *40* (23), 7367−7373.

(13) Shi, J.; Fujisawa, S.; Nakai, S.; Hosomi, M. Biodegradation of natural and synthetic estrogens by nitrifying activated sludge and ammonia-oxidizing bacterium *Nitrosomonas europaea*. *Water Res.* **2004**, *38* (9), 2322−9.

(14) Fernandez-Fontaina, E.; Omil, F.; Lema, J. M.; Carballa, M. Influence of nitrifying conditions on the biodegradation and sorption of emerging micropollutants. *Water Res.* **2012**, *46* (16), 5434−5444.

(15) Falas, P.; Baillon-Dhumez, A.; Andersen, H. R.; Ledin, A.; la Cour Jansen, J. Suspended biofilm carrier and activated sludge removal of acidic pharmaceuticals. *Water Res.* **2012**, *46* (4), 1167−75.

(16) Keener, W. K.; Arp, D. J. Transformations of aromatic compounds by *Nitrosomonas europaea*. *Appl. Environ. Microbiol.* **1994**, *60* (6), 1914−1920.

(17) Hooper, A. B.; Vannelli, T.; Bergmann, D. J.; Arciero, D. M. Enzymology of the oxidation of ammonia to nitrite by bacteria. In *Beijerinck Centennial Symposium on Microbial Physiology and Gene Regulation: Emerging Principles and Applications, The Hague, Netherlands, Dec, 1995*; Kluwer Academic Publ: The Hague, Netherlands, 1995; pp 59−67.

(18) Skotnicka-Pitak, J.; Khunjar, W. O.; Love, N. G.; Aga, D. S. Characterization of metabolites formed during the biotransformation of 17α-ethinylestradiol by *Nitrosomonas europaea* in batch and continuous flow bioreactors. *Environ. Sci. Technol.* **2009**, *43* (10), 3549−3555.

(19) Hooper, A. B.; Vannelli, T.; Bergmann, D. J.; Arciero, D. M. Enzymology of the oxidation of ammonia to nitrite by bacteria. *Antonie Van Leeuwenhoek* **1997**, *71* (1−2), 59−67.

(20) Arp, D. J.; Stein, L. Y. Metabolism of inorganic N compounds by ammonia-oxidizing bacteria. *Crit. Rev. Biochem. Mol. Biol.* **2003**, *38* (6), 471−495.

(21) Arp, D. J.; Chain, P. S. G.; Klotz, M. G. The impact of genome analyses on our understanding of ammonia-oxidizing bacteria. *Annu. Rev. Microbiol.* **2007**, *61*, 503−528.

(22) Taher, E.; Chandran, K. High-rate, high-yield production of methanol by ammonia-oxidizing bacteria. *Environ. Sci. Technol.* **2013**, *47* (7), 3167−3173.

(23) Ginestet, P.; Audic, J. M.; Urbain, V.; Block, J. C. Estimation of nitrifying bacterial activities by measuring oxygen uptake in the presence of the metabolic inhibitors allylthiourea and azide. *Appl. Environ. Microbiol.* **1998**, *64* (6), 2266−2268.

(24) *Nitrogen, Ammonia Salicylate Method*, 5th ed.; Hach: Loveland, CO, 2008.

(25) *Standard Methods for the Examination of Water and Wastewater*, 20th ed.; APHA; AWWA; WEF: Washington, DC; Denver, CO; Alexandria, VA, 1999.

(26) Rotthauwe, J. H.; Witzel, K. P.; Liesack, W. The ammonia monooxygenase structural gene amoA as a functional marker: Molecular fine-scale analysis of natural ammonia-oxidizing populations. *Appl. Environ. Microbiol.* **1997**, *63* (12), 4704−4712.

(27) Park, H.; Rosenthal, A.; Jezek, R.; Ramalingam, K.; Fillos, J.; Chandran, K. Impact of inocula and growth mode on the molecular microbial ecology of anaerobic ammonia oxidation (anammox) bioreactor communities. *Water Res.* **2010**, *44* (17), 5005−5013.

(28) Kindaichi, T.; Kawano, Y.; Ito, T.; Satoh, H.; Okabe, S. Population dynamics and in situ kinetics of nitrifying bacteria in autotrophic nitrifying biofilms as determined by real-time quantitative PCR. *Biotechnol. Bioeng.* **2006**, *94* (6), 1111−1121.

(29) Graham, D. W.; Knapp, C. W.; Van Vleck, E. S.; Bloor, K.; Lane, T. B.; Graham, C. E. Experimental demonstration of chaotic instability in biological nitrification. *ISME J.* **2007**, *1* (5), 385−393.
(30) Ferris, M. J.; Muyzer, G.; Ward, D. M. Denaturing gradient gel electrophoresis profiles of 16S rRNA-defined populations inhabiting a hot spring microbial mat community. *Appl. Environ. Microbiol.* **1996**, *62* (2), 340−346.
(31) Urase, T.; Kikuta, T. Separate estimation of adsorption and degradation of pharmaceutical substances and estrogens in the activated sludge process. *Water Res.* **2005**, *39* (7), 1289−300.
(32) Helbling, D. E.; Johnson, D. R.; Honti, M.; Fenner, K. Micropollutant biotransformation kinetics associate with WWTP process parameters and microbial community characteristics. *Environ. Sci. Technol.* **2012**, *46* (19), 10579−10588.
(33) Alvarez-Cohen, L.; Speitel, G. E. Kinetics of aerobic cometabolism of chlorinated solvents. *Biodegradation* **2001**, *12* (2), 105−126.
(34) Criddle, C. S. The kinetics of cometabolism. *Biotechnol. Bioeng.* **1993**, *41* (11), 1048−1056.
(35) Ely, R. L.; Williamson, K. J.; Guenther, R. B.; Hyman, M. R.; Arp, D. J.; Cometabolic, A. Kinetics model incorporating enzyme-inhibition, inactivation, and recovery. 1. Model development, analysis, and testing. *Biotechnol. Bioeng.* **1995**, *46* (3), 218−231.
(36) Henze, M.; Gujer, W.; Mino, T.; Loosdrecht, M. V. *Activated Sludge Models ASM1, ASM2, ASM2d, and ASM3*; IWA Pub.: London, 2000; pp vi, 121.
(37) Chandran, K.; Smets, B. F. Single-step nitrification models erroneously describe batch ammonia oxidation profiles when nitrite oxidation becomes rate limiting. *Biotechnol. Bioeng.* **2000**, *68* (4), 396−406.
(38) Hiatt, W. C.; Grady, C. P. L. An updated process model for carbon oxidation, nitrification, and denitrification. *Water Environ. Res.* **2008**, *80* (11), 2145−2156.
(39) Grady, C. P. L.; Diagger, G. T.; Lim, H. C. *Biological Wastewater Treatment*; Marcel Dekker: New York, 1999.
(40) Orhon, D.; Artan, N. *Modelling of Activated Sludge Systems*; Techmonic Publishing Company: Lancaster, 1994.
(41) Bedard, C.; Knowles, R. Physiology, biochemistry, and specific inhibitors of CH4, NH4+ and CO oxidation by methanotrophs and nitrifiers. *Microbiol. Rev.* **1989**, *53* (1), 68−84.
(42) Dytczak, M. A.; Londry, K. L.; Oleszkiewicz, J. A. Activated sludge operational regime has significant impact on the type of nitrifying community and its nitrification rates. *Water Res.* **2008**, *42* (8−9), 2320−2328.
(43) Schramm, A.; De Beer, D.; Gieseke, A.; Amann, R. Microenvironments and distribution of nitrifying bacteria in a membrane-bound biofilm. *Environ. Microbiol.* **2000**, *2* (6), 680−686.
(44) Sathyamoorthy, S.; Ramsburg, C. A. Assessment of quantitative structural property relationships for prediction of pharmaceutical sorption during biological wastewater treatment. *Chemosphere* **2013**, *92* (6), 639−646.
(45) Maurer, M.; Escher, B. I.; Richle, P.; Schaffner, C.; Alder, A. C. Elimination of beta-blockers in sewage treatment plants. *Water Res.* **2007**, *41* (7), 1614−22.
(46) Gaulke, L. S.; Strand, S. E.; Kalhorn, T. F.; Stensel, H. D. 17α-ethinylestradiol transformation via abiotic nitration in the presence of ammonia oxidizing bacteria. *Environ. Sci. Technol.* **2008**, *42* (20), 7622−7627.
(47) Wick, A.; Fink, G.; Joss, A.; Siegrist, H.; Ternes, T. A. Fate of beta blockers and psycho-active drugs in conventional wastewater treatment. *Water Res.* **2009**, *43* (4), 1060−74.
(48) Burnham, K. P.; Anderson, D. R. *Model Selection and Multimodel Inference: A Practical Information-Theoretic Approach*; Springer-Verlag: New York, 2002.
(49) Harms, G.; Layton, A. C.; Dionisi, H. M.; Gregory, I. R.; Garrett, V. M.; Hawkins, S. A.; Robinson, K. G.; Sayler, G. S. Real-time PCR quantification of nitrifying bacteria in a municipal wastewater treatment plant. *Environ. Sci. Technol.* **2003**, *37* (2), 343−351.
(50) Ahn, J. H.; Yu, R.; Chandran, K. Distinctive microbial ecology and biokinetics of autotrophic ammonia and nitrite oxidation in a partial nitrification Bioreactor. *Biotechnol. Bioeng.* **2008**, *100* (6), 1078−1087.
(51) Bailey, J. E.; Ollis, D. F., *Biochemical Engineering Fundamentals*. McGraw-Hill: 1986.
(52) Radniecki, T. S.; Dolan, M. E.; Semprini, L. Physiological and transcriptional responses of *Nitrosomonas europaea* to toluene and benzene inhibition. *Environ. Sci. Technol.* **2008**, *42* (11), 4093−4098.
(53) Ely, R. L.; Williamson, K. J.; Hyman, M. R.; Arp, D. J. Cometabolism of chlorinated solvents by nitrifying bacteria: Kinetics, substrate interactions, toxicity effects, and bacterial response. *Biotechnol. Bioeng.* **1997**, *54* (6), 520−534.
(54) Kocamemi, B. A.; Cecen, F. Cometabolic degradation of TCE in enriched nitrifying batch systems. *J. Hazard. Mater.* **2005**, *125* (1−3), 260−265.
(55) Kocamemi, B. A.; Cecen, F. Cometabolic degradation and inhibition kinetics of 1,2-dichloroethane (1,2-DCA) in suspended-growth nitrifying systems. *Environ. Technol.* **2010**, *31* (3), 295−305.
(56) Kocamemi, B. A.; Cecen, F. Biological removal of the xenobiotic trichloroethylene (TCE) through cometabolism in nitrifying systems. *Bioresour. Technol.* **2010**, *101* (1), 430−433.
(57) Sathyamoorthy, S. Influence of sorption and nitrification processes on pharmaceutical attenuation during biological wastewater treatment. Doctoral Dissertation, Tufts University, Medford, MA, 2013.
(58) Mota, C.; Ridenoure, J.; Cheng, J. Y.; de los Reyes, F. L. High levels of nitrifying bacteria in intermittently aerated reactors treating high ammonia wastewater. *FEMS Microbiol. Ecol.* **2005**, *54* (3), 391−400.
(59) Munz, G.; Lubello, C.; Oleszkiewicz, J. A. Factors affecting the growth rates of ammonium and nitrite oxidizing bacteria. *Chemosphere* **2011**, *83* (5), 720−725.
(60) Marsili-Libelli, S.; Ratini, P.; Spagni, A.; Bortone, G. Implementation, study, and calibration of a modified ASM2d for the simulation of SBR processes. *Water Sci. Technol.* **2001**, *43* (3), 69−76.
(61) Manser, R.; Gujer, W.; Siegrist, H. Consequences of mass transfer effects on the kinetics of nitrifiers. *Water Res.* **2005**, *39* (19), 4633−4642.
(62) Chandran, K.; Hu, Z. Q.; Smets, B. F. A critical comparison of extant batch respirometric and substrate depletion assays for estimation of nitrification biokinetics. *Biotechnol. Bioeng.* **2008**, *101* (1), 62−72.
(63) Sin, G.; Kaelin, D.; Kampschreur, M. J.; Takacs, I.; Wett, B.; Gernaey, K. V.; Rieger, L.; Siegrist, H.; van Loosdrecht, M. C. M. Modelling nitrite in wastewater treatment systems: a discussion of different modelling concepts. *Water Sci. Technol.* **2008**, *58* (6), 1155−1171.
(64) Munz, G.; Mori, G.; Vannini, C.; Lubello, C. Kinetic parameters and inhibition response of ammonia- and nitrite-oxidizing bacteria in membrane bioreactors and conventional activated sludge processes. *Environ. Technol.* **2010**, *31* (14), 1557−1564.
(65) Kampschreur, M. J.; Picioreanu, C.; Tan, N.; Kleerebezem, R.; Jetten, M. S. M.; van Loosdrecht, M. C. M. Unraveling the source of nitric oxide emission during nitrification. *Water Environ. Res.* **2007**, *79* (13), 2499−2509.
(66) Jones, R. M.; Dold, P.; Takacs, I.; Chapman, K.; Wett, B.; Murthy, S.; O'Shaughnessy, M. Simulation for operation and control of reject water treatment processes. In *WEFTEC 2007*; Water Environment Federation: San Diego, CA, 2007.